AMERICAN SOCIETY FOR MICROBIOLOGY | Applied and Environmental Microbiology®

GENETICS AND MOLECULAR BIOLOGY

A Family of Secretory Proteins Is Associated with Different Morphotypes in *Cryptococcus neoformans*

Rachana Gyawali, Srijana Upadhyay, Joshua Way, Xiaorong Lin

Department of Biology, Texas A&M University, College Station, Texas, USA

ABSTRACT *Cryptococcus neoformans*, an opportunistic human fungal pathogen, can undergo a yeast-to-hypha transition in response to environmental cues. This morphological transition is associated with changes in the expression of cell surface proteins. The *Cryptococcus* cell surface and secreted protein Cfl1 was the first identified adhesin in the Basidiomycota. Cfl1 has been shown to regulate morphology, biofilm formation, and intercellular communication. Four additional homologs of *CFL1* are harbored by the *Cryptococcus* genome: *DHA1*, *DHA2*, *CPL1*, and *CFL105*. The common features of this gene family are the conserved C-terminal SIGC domain and the presence of an N-terminal signal peptide. We found that all these Cfl1 homolog proteins are indeed secreted extracellularly. Interestingly, some of these secretory proteins display cell type-specific expression patterns: Cfl1 is hypha specific, Dha2 is yeast specific, and Dha1 (delayed hypersensitivity antigen 1) is expressed in all cell types but is particularly enriched at basidia. Interestingly, Dha1 is induced by copper limitation and suppressed by excessive copper in the medium. This study further attests to the physiological heterogeneity of the *Cryptococcus* mating colony, which is composed of cells with heterogeneous morphotypes. The differential expression of these secretory proteins contributes to heterogeneity, which is beneficial for the fungus to adapt to changing environments.

IMPORTANCE Heterogeneity in physiology and morphology is an important bet-hedging strategy for nonmobile microbes such as fungi to adapt to unpredictable environmental changes. *Cryptococcus neoformans*, a ubiquitous basidiomycetous fungus, is known to switch from the yeast form to the hypha form during sexual development. However, in a mating colony, only a subset of yeast cells switch to hyphae, and only a fraction of the hyphal subpopulation will develop into fruiting bodies, where meiosis and sporulation occur. Here, we investigated a basidiomycete-specific secretory protein family. We found that some of these proteins are cell type specific, thus contributing to the heterogeneity of a mating colony. Our study also demonstrates the importance of examining the protein expression pattern at the individual-cell level in addition to population gene expression profiling for the investigation of a heterogeneous community.

KEYWORDS dimorphism, morphogenesis, morphotype, secretory proteins, sexual reproduction

Received 26 October 2016 **Accepted** 19 December 2016

Accepted manuscript posted online 30 December 2016

Citation Gyawali R, Upadhyay S, Way J, Lin X. 2017. A family of secretory proteins is associated with different morphotypes in *Cryptococcus neoformans*. Appl Environ Microbiol 83:e02967-16. https://doi.org/10.1128/AEM.02967-16.

Editor Janet L. Schottel, University of Minnesota

Address correspondence to Xiaorong Lin, xlin@bio.tamu.edu.

Adhesins are cell surface proteins that are required for microbes to adhere to the substrate as well as to other cells (1–3). Adhesins in pathogenic fungi play a role in a wide variety of functions, such as host-pathogen interactions, biofilm formation, filamentation, and mating (2, 4, 5). The expression of adhesins is responsive to environmental cues (1). For instance, adhesins of *Saccharomyces* (Flo proteins) are activated during nitrogen or carbon source starvation, and they are required for cell-cell adherence and cell-substrate adherence (6–8). Many fungal adhesins show a cell type-specific

expression pattern. For instance, *Candida albicans* Hwp1 and Hwp2 are hypha specific, and they are also upregulated in opaque cells during mating. Hwp1 and Hwp2 are required for *Candida* adhesion to host cells and the formation of biofilms (9–11). On the other hand, *Candida* Ywp1 is a yeast cell-specific cell wall protein that inhibits adhesion (12, 13). Candidalysin, the hypha-specific secreted protein, is required for *Candida* to cause damage to epithelial cells, but it does not have any effect on *Candida* hyphal morphogenesis *per se* (14). Bad1, the adhesin and an important virulence factor characterized in *Blastomyces dermatitidis*, is yeast specific (15). Understanding the regulation of cell surface proteins thus can help us understand fungal development and how the fungus interacts with its environment and the host.

Cell flocculin 1 (Cfl1), a hypha-specific protein of *Cryptococcus*, was the first adhesin identified in the phylum Basidiomycota (16–18). *CFL1* is one of the most induced genes during *Cryptococcus* sexual development (17, 18). The *Cryptococcus* adhesin Cfl1 is unique in that it does not contain a common domain structure present in the known ascomycete fungal adhesins, such as a C-terminal glycosylphosphatidylinositol (GPI) anchor, an N-terminal carbohydrate or peptide binding domain, or the middle domain containing serine/threonine-rich repeats (6, 19). However, consistent with the function of adhesins, the overexpression of Cfl1 leads to a wrinkled colony morphology as well as increased flocculation (17). Furthermore, Cfl1 is a secretory protein, and its secretion is required for its adhesion function. Cfl1 is both cell wall associated and released. Released Cfl1 acts as a signal to regulate colony morphology in autocrine and paracrine manners (18). Therefore, cells expressing Cfl1 can induce the expression of endogenous Cfl1 in neighboring cells, which leads to the formation of biofilm and the production of hyphae (18).

The domain organization of Cfl1 shows that it contains an N-terminal EGF motif and an amylogenic region that has a predicted function in cell-cell adhesion (18). The C-terminal region containing 80 amino acid residues is highly conserved among Cfl1 homologs across different basidiomycetous species and is named the SIGC domain (signal C-terminal domain) (18). Interestingly, the genome of *Cryptococcus neoformans* var. *neoformans* has four additional conserved Cfl1 homologs. The aim of this study is to characterize these homologs and to understand their role in the development of *Cryptococcus neoformans*.

RESULTS

Identification of genes encoding Cfl1 homologs in the *Cryptococcus* genome. Based on data from a previous study (17), the *Cryptococcus neoformans* genome has four additional homologs of Cfl1. A BLAST search of Cfl1 against two serotype D translated genomes (B3501 and JEC21) using FungiDB led to the identification of these four additional *CFL1* (CNA07720 and CNAG_00795 for serotype A) homologs as *DHA1* (CND04870 and CNAG_07422 for serotype A), *DHA2* (CNM00910 and CNAG_06082 for serotype A), *CPL1* (CNC04160 and CNAG_02797 for serotype A), and *CFL105* (CNG01330 and CNAG_03454 for serotype A). Two more hits with lower homology were found in the serotype A H99 genome, but these two genes were absent in the serotype D genomes and thus were not included in this study. All identified Cfl1 homologs have an N-terminal signal peptide and are predicted to be secretory proteins based on the SignalP and WoLFPSORT programs. The relative length of the signal peptide shown in Fig. 1A was drawn based on the length of the signal peptide predicted by SignalP. All Cfl1 homologs have the C-terminal SIGC domain, which is the most conserved region (Fig. 1A). Among all Cfl1 homologs, Dha1 and Dha2 are most similar, sharing 72% identities and 83% similarities. This suggests that Dha1 and Dha2 might be paralogs. In comparison, the identities shared between other Cfl1 homologs are $<$40%. Structural prediction of the Cfl1 homologs by PHYRE2 did not reveal any features suggestive of potential function. It was shown previously that the Dha1 protein can elicit a delayed-type hypersensitivity (DTH) reaction in mice based on a mouse footpad swelling assay (20). *CPL1* has been shown to affect capsule formation, and the gene deletion mutants had reduced virulence in a systematic study of about 1,200 gene deletion mutants (21).

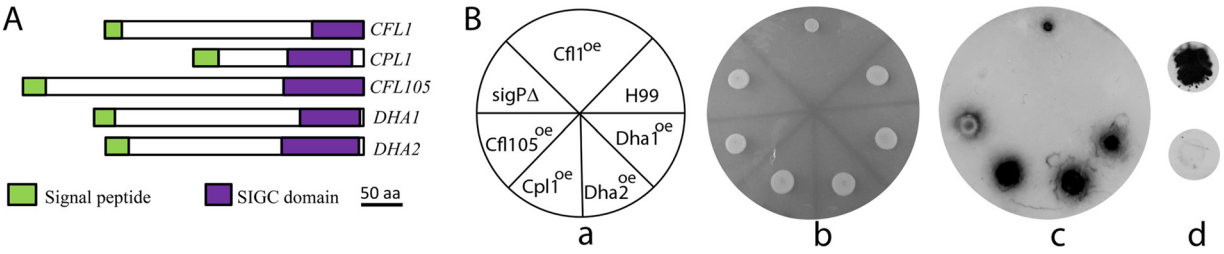

FIG 1 (A) Schematic diagram of the amino acid sequence alignment of *CFL1* homologs. The SignalP 4.1 server was used for the prediction of the signal peptide and the location of the signal peptide cleavage site. The position of the SIGC domain among the homologs was predicted based on a BLAST search of the *CFL1* SIGC domain against each homolog. All of the Cfl1 homologs have an N-terminal signal peptide for secretion and the C-terminal SIGC domain. The similarity in sequence among the homologs lies mostly in the SIGC domain. aa, amino acids. (B) Cfl1 homologs are secretory proteins and are released extracellularly. The P_{CTR4}-*CFL1*::mCherry (Cfl1^{oe}), P_{CTR4}-*DHA1*::mCherry (Dha1^{oe}), P_{CTR4}-*DHA2*::mCherry (Dha2^{oe}), P_{CTR4}-*CPL1*::mCherry (Cpl1^{oe}), and P_{CTR4}-*CFL105*::mCherry (Cfl105^{oe}) strains were grown overnight in liquid YPD medium. Cells of the same OD (OD_{600} = 3) were spotted onto V8 medium with BCS. Proteins released from the colony onto the membrane were detected by using the mCherry antibody. (a) Layout of the strains grown on V8 agar medium. (b) Colony images of the strains on V8 agar medium. Because Cfl1 is known to be secreted abundantly during mating, Cfl1-overexpressing cells were inoculated 3 days later than the other strains to avoid potential interference of the signal from Cfl1^{oe} cells with signals from other cells. (c) Colony immunoblotting to detect secreted products from all the strains overexpressing Cfl1 homologs. No signal was detected from WT H99 cells or SigPΔ-Cfl1^{oe} cells with the Cfl1 signal peptide deleted. (d) Colony immunoblotting of Cfl1^{oe} cells (top) and SigPΔ-Cfl1^{oe} cells with a signal peptide deletion (bottom). Here, both strains were cultured for 5 days before the membrane was laid over the colonies.

In a recent study, Cpl1 was shown to be secreted into the culture supernatant and was also detected in serum of mice infected with *Cryptococcus neoformans* (22). The role of these homologs in *Cryptococcus* development has not been studied.

All Cfl1 homologs are secreted proteins. Cfl1 is known to be released extracellularly (18). We also know that mCherry-tagged Cfl1 at its C terminus is functional (18). To test if the homologs of Cfl1 are released extracellularly like Cfl1, we applied the same approach, tagged all the Cfl1 homologs with mCherry, and placed their expression under the control of the inducible promoter of the copper transporter gene *CTR4* (18). We then performed a colony immunoblot assay with these strains cultured under copper-limiting conditions where the expression of these genes was induced. As expected, we detected extracellularly released Cfl1 in this assay (Fig. 1B). Because Cfl1 was secreted abundantly (Fig. 1Bd), we spotted Cfl1-overexpressing cells 3 days later than for the other strains so that the signal from Cfl1^{oe} cells would not interfere with signals from other colonies (hence, the Cfl1^{oe} colony is smaller in Fig. 1B). We did not detect signals from strain LW295 (Cfl1-sigPΔ), where the Cfl1 signal peptide was deleted, or from the wild-type (WT) strain without the mCherry tag (Fig. 1B), as expected. In contrast, we detected signals from colonies where the four Cfl1 homologs were tagged with mCherry by colony immunoblotting (Fig. 1B). This result indicates that all four homologs of Cfl1 are indeed released into the milieu like Cfl1.

Impact of overexpression of the Cfl1 homologs on colony morphology. We previously demonstrated that the overexpression of Cfl1 promotes cell-cell adhesion, as reflected by the wrinkled colony morphology of Cfl1^{oe} cells (17, 18). On yeast extract-peptone-dextrose (YPD) medium, P_{CTR4}-*CFL1*-mCherry cells formed a complex/wrinkled colony when cultured under inducing conditions in the presence of the copper chelator bathocuproinedisulfonic acid (BCS), while the strain formed a smooth colony under repressing conditions in the presence of copper (see Fig. S1A in the supplemental material). This observation was expected based on data from our previous studies (16–18). P_{CTR4}-*CFL105*-mCherry strain (Cfl105^{oe}), P_{CTR4}-*DHA1*-mCherry strain (Dha1^{oe}), and P_{CTR4}-*CPL1*-mCherry strain (Cpl1^{oe}) colonies showed modestly increased wrinkledness in colony morphology in the presence of BCS but to a lesser degree than with the Cfl1^{oe} colony under the same inducing conditions (Fig. S1A). On yeast nitrogen base (YNB) medium, the Cfl1^{oe} colony and the Cfl105^{oe} colony showed obviously increased wrinkledness in colony morphology in the presence of BCS (Fig. S1B). Consistently, the Cfl1^{oe} and Cfl105^{oe} strains also showed increased invasive growth on YNB medium plus BCS (Fig. S1B). Any enhancement in invasive growth or wrinkledness in colonies disappeared when these strains were cultured in the presence of copper, indicating

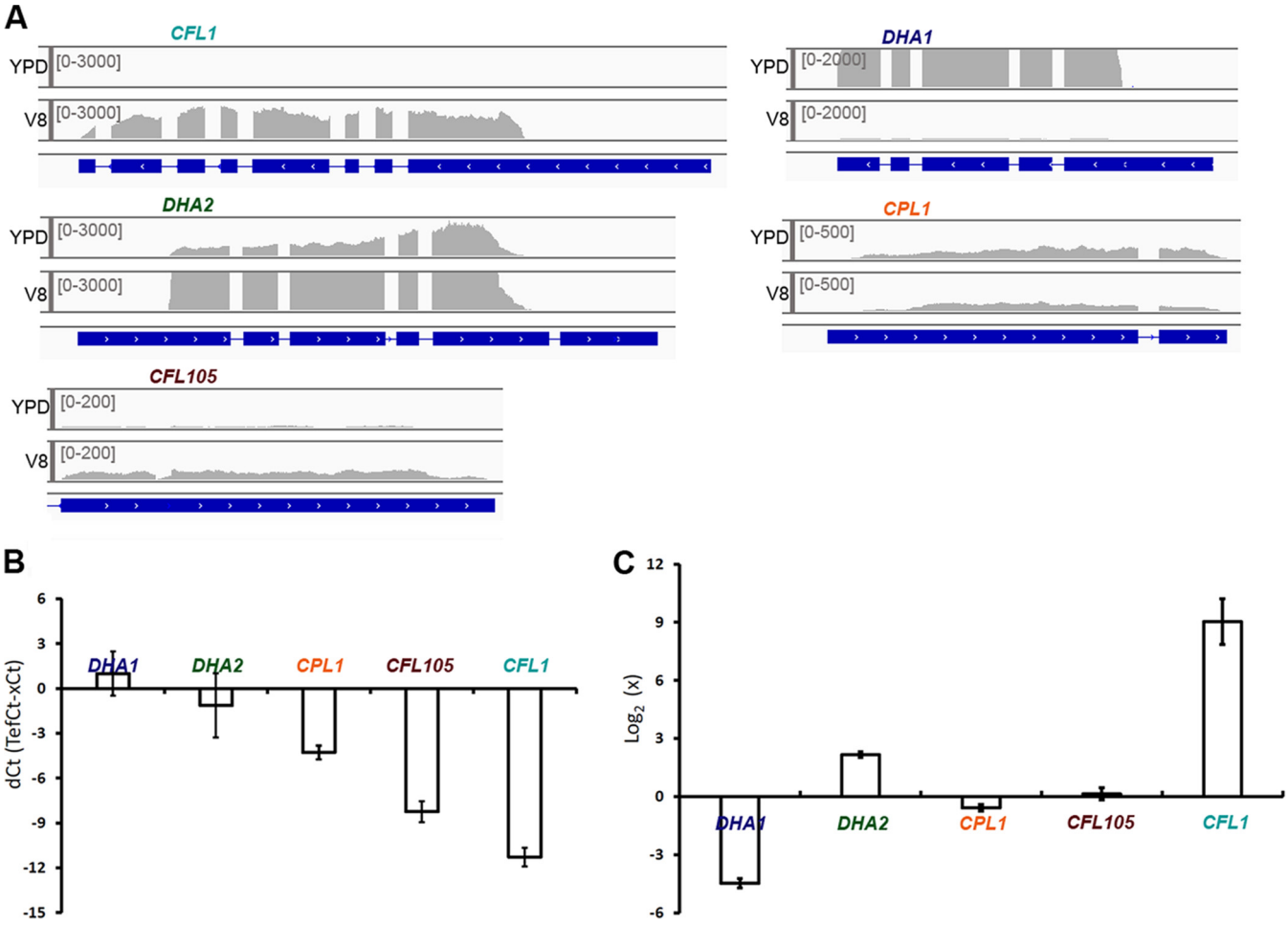

FIG 2 (A) Transcript levels (fragments per kilobase per million) of the *CFL1* homologs when the wild-type XL280 strain was cultured in YPD or V8 medium for 24 h based on RNA-seq data (23). IGV software was used for viewing the transcripts. The read count scale was set to a different threshold value for each gene so that the transcript level of each gene could be easily visualized. (B) Relative transcript levels of *CFL1* homologs based on RT-PCR. RNA samples for yeast-phase growth were collected from WT XL280 cells cultured in liquid YPD medium overnight. The RT-PCR graph shows the delta cycle threshold (dCt) values of the *CFL1* homologs. The dCT value was calculated based on a comparison of the Ct value of the respective gene with that of the *TEF1* gene. (C) RNA samples for the mating samples were collected after WT XL280 cells were cultured on V8 agar medium for 24 h. The relative transcript levels of the genes on the mating medium was compared to their transcript levels in YPD medium.

that the effect was due to increased gene expression. Because different adhesins adhere to cells or substrates differently, we further examined the impact of their overexpression on cell adherence to glass. We cultured these strains in RPMI medium with BCS or copper. We then examined the glass slides after washing. We found that only Cfl1^{oe} and Cfl105^{oe} showed strong adherence to glass, while Dha1^{oe} and Cpl1^{oe} showed slightly increased adherence to glass compared to the wild-type control (Fig. S1C). Taken together, these results suggest that Cfl105 and Cfl1 promote adherence under various conditions.

Expression profile of *CFL1* homologs during vegetative growth and sexual development. To understand their role in *Cryptococcus* development, we examined the expression pattern of *CFL1* homologs in wild-type strain XL280 during yeast-phase growth in YPD medium and during sexual development on V8 medium by analyzing transcriptome sequencing (RNA-seq) data that we recently reported (23). During yeast-phase growth in YPD medium, *CFL1* showed the lowest transcript level, whereas *DHA1* showed the highest transcript level (Fig. 2A). This pattern was consistent with our quantitative real-time PCR (RT-PCR) results (Fig. 2B). The high expression level of *DHA1* during yeast growth observed here was consistent with data from a previous study where the Dha1 protein was easily detected in the supernatant of *Cryptococcus* yeast

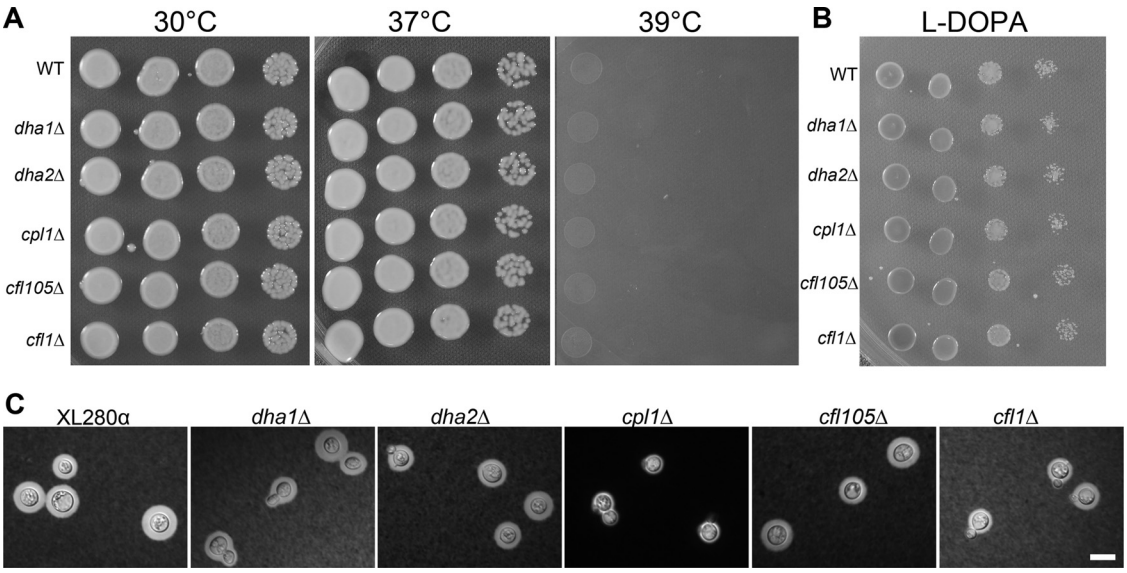

FIG 3 Effect of gene deletion on thermotolerance, melanin production, and capsule production. Cells of wild-type strain XL280, the *dha1*Δ mutant, the *dha2*Δ mutant, the *cpl1*Δ mutant, the *cfl105*Δ mutant, and the *cfl1*Δ mutant of the same OD (OD_{600} = 3) were serially diluted (10 times) and spotted onto YPD or L-DOPA agar medium. To examine capsule, cells were cultured in liquid RPMI medium. (A) To test thermotolerance, cells on YPD medium were incubated at 30°C, 37°C, or 39°C. (B) To test melanization, cells on L-DOPA medium were incubated at 22°C in the dark. (C) India ink exclusion assay of capsule production of cells cultured in RPMI medium at 37°C with 5% CO_2. Bar, 10 μm.

cultures (20). The transcript level of *DHA2* was ranked second in YPD medium, followed by *CPL1*, *CFL105*, and *CFL1* (Fig. 2A and B).

Cryptococcus can undergo unisexual development on mating-inducing media such as V8 juice agar medium (24, 25). During unisexual development on V8 medium, at 24 h postinoculation, the transcript levels of *CFL1* and *DHA2* were significantly higher than those of other genes based on RNA-seq data (Fig. 2A). The increase in the transcript levels of these two genes on V8 medium compared to those in YPD medium was confirmed with our RT-PCR results (Fig. 2B and C). The findings indicated that the *CFL1* and *DHA2* transcript levels drastically increased during unisexual development on V8 medium compared to those in YPD medium (Fig. 2A and C). The high level of *CFL1* transcripts during unisexual development was expected given that Cfl1 is a hypha-specific protein (17). Because *DHA2* was also significantly induced during unisexual development on V8 medium, we speculate that *DHA2* might also be specifically induced in the hyphal subpopulation like *CFL1*. On the other hand, no drastic change in transcript levels was observed for *CPL1* or *CFL105* during sexual development on V8 medium compared to yeast growth in YPD medium. In contrast, the *DHA1* transcript level was drastically reduced on V8 medium, suggesting that *DHA1* might encode a yeast-specific product. The expression data for some of these *CFL1* homolog genes showed that some of these genes had higher transcript levels during yeast-phase growth, while some were induced during sexual development. Thus, we hypothesize that some of these homologs, particularly Dha1, Dha2, and Cfl1, likely play a role in *Cryptococcus* development.

Impact of the deletion of *CFL1* homologs on *Cryptococcus* classic virulence traits. To examine if Cfl1 homologs play any role in *Cryptococcus* virulence traits and morphology, we deleted these genes in the serotype D strain XL280α background. We also obtained the corresponding gene deletion mutants in the mating type **a** background and verified the Mendelian segregation of the gene deletion. We then used these deletion mutants for phenotypic assays, including assays for thermotolerance, melanization, and capsule production. Mutants of either the **a** or the α mating type behaved similarly. Deletion of most of the *CFL1* homologs in XL280 did not have any apparent effect on thermotolerance or melanin production (Fig. 3A and B). Likewise, no

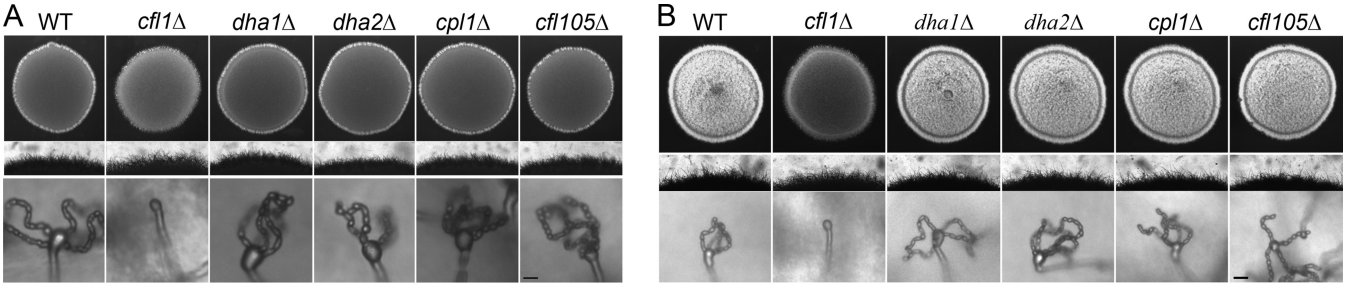

FIG 4 Effect of gene deletion mutants on unisexual and bisexual reproduction. Cells of wild-type strain XL280, the *dha1*Δ mutant, the *dha2*Δ mutant, the *cpl1*Δ mutant, the *cfl105*Δ mutant, and the *cfl1*Δ mutant (all of the α mating type) at the same cell density were spotted onto V8 agar medium and incubated in the dark at 22°C for 5 days either alone for unisexual reproduction (A) or mixed together with the corresponding mutant in the mating type **a** background for bisexual reproduction (B). The white fluffy appearance of the colony reflects the production of aerial hyphae. Deletion of *CFL1* led to reduced aerial hypha formation in both unisexual and bisexual reproduction. Sporulation is significantly reduced and delayed; however, the cells eventually sporulate (see Fig. S3 in the supplemental material). Bars, 10 μm.

defect in melanization or growth at high temperatures was observed for the gene deletion mutants made in the serotype A strain H99 background (see Fig. S2 in the supplemental material). We also did not observe an obvious impact on capsule production by the disruption of most of the *CFL1* homologs except *CPL1* in the XL280 background (Fig. 3C). A smaller capsule size of the *cpl1*Δ mutant in the H99 background was also observed (Fig. S2). This finding is consistent with a previous observation of the *cpl1*Δ mutant made in the H99 background (21).

There is no significant impact on *Cryptococcus* development when the *CFL1* homologs are deleted. Given that Cfl1 plays an important role in promoting the yeast-to-hypha morphological transition in *Cryptococcus*, we decided to examine if the Cfl1 homologs also play a role in filamentation and sporulation during cryptococcal development. *Cryptococcus* can undergo filamentation and sporulation both during **a**-α bisexual reproduction and during unisexual reproduction with cells of one mating type (24–26). We chose to use strains in the wild-type XL280α background for such investigations, as XL280 has been widely used for morphogenesis studies (27). We first examined the effect of the deletion of these genes during unisexual development where α cells alone were cultured under mating-inducing conditions (V8 juice agar medium). Deletion of the *CFL1* gene substantially reduced aerial hypha formation (Fig. 4A), as shown previously (18). Even though no spores could be detected in the *cfl1*Δ mutant when the WT strain had already produced spores, the *cfl1*Δ mutant eventually sporulated and formed long chains of spores (see Fig. S3 in the supplemental material). The delay in sporulation shown by the *cfl1*Δ mutant was rescued by *CFL1* reconstitution (Fig. S3). Surprisingly, no obvious defect in filamentation or sporulation was observed for the *dha1*Δ mutant, the *dha2*Δ mutant, the *cpl1*Δ mutant, or the *cfl105*Δ mutant (Fig. 4A). We further obtained gene deletion mutants in the mating type **a** background by dissecting the meiotic progeny from a cross between the gene deletion **a** strain and the congenic WT **a** strain (27). Again, there was a lack of obvious defects in the filamentation or sporulation of the corresponding mutants in the mating type **a** background. These results indicate that these genes, with the exception of *CFL1*, are not required for the morphological transition during self-filamentation.

To examine the effect of the disruption of *CFL1* homolog genes on bisexual mating, we performed crosses of mutant α cells with the corresponding mutant **a** cells. As expected, the cross of *cfl1*Δ $\alpha \times$ *cfl1*Δ **a** showed reduced production of aerial hyphae and spores. Although there was a delay in sporulation, the *cfl1*Δ $\alpha \times$ *cfl1*Δ **a** cross eventually formed long chains of spores within 14 days (see Fig. S3 in the supplemental material). However, no apparent defect in bilateral bisexual mating was detected for any of the other gene deletion mutants (Fig. 4B).

The fact that the deletion of *DHA2* did not yield any obvious phenotype during cryptococcal development was surprising given that its transcript level was drastically induced during mating. One possible explanation for this is that Dha2 might not

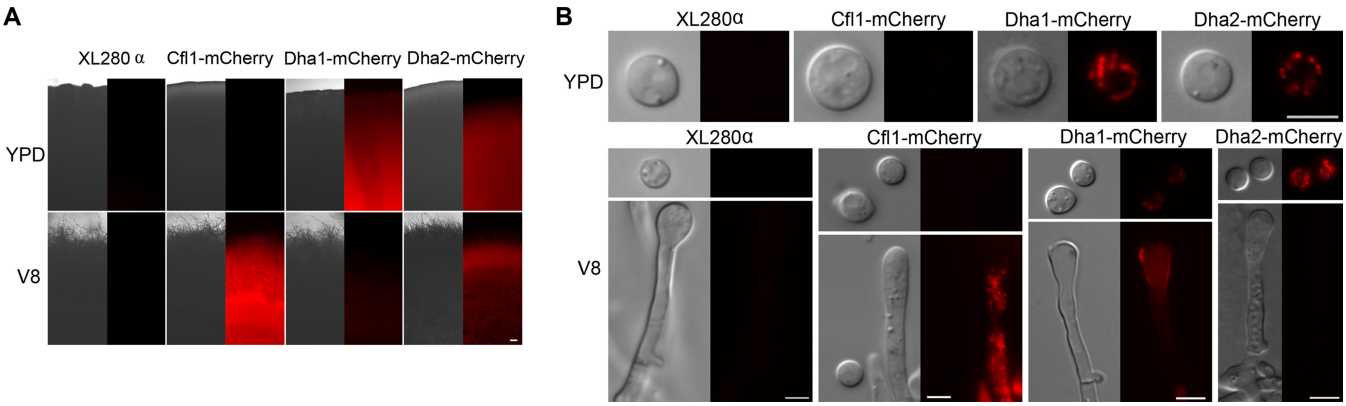

FIG 5 Protein expression pattern of Cfl1, Dha1, and Dha2 during yeast-phase growth and during cryptococcal development. Each protein is fused with mCherry at its C terminus, and gene expression was driven by its native promoter. (A) Colony images of unlabeled wild-type strain XL280, the P_{CFL1}-*CFL1*-mCherry strain, the P_{DHA1}-*DHA1*-mCherry strain, and the P_{DHA2}-*DHA2*-mCherry strain grown in YPD medium and on V8 medium. Bar, 100 μm. (B) Expression and subcellular localization of Cfl1, Dha1, and Dha2 in yeast cells during growth in YPD medium and on V8 medium. Shown are differential interference contrast and fluorescence images of cells of unlabeled wild-type strain XL280, the P_{CFL1}-*CFL1*-mCherry strain, the P_{DHA1}-*DHA1*-mCherry strain, and the P_{DHA2}-*DHA2*-mCherry strain in YPD medium (yeast cells only) and on V8 medium (yeast cells and hyphae). Bar, 5 μm.

directly play a role in hypha production or hyphal elongation *per se*, but its production is associated with cryptococcal development. For instance, it may sense or respond to other environmental cues that are typically present under mating conditions. This is the case with the secreted protein *ECE1* of *Candida albicans*. *ECE1* is highly expressed by *Candida* hyphal cells during epithelial infection, but the deletion of *ECE1* does not affect hypha morphology, adherence, or *Candida* invasion of human epithelial cells (14). Interestingly, the secretion of the encoded protein is crucial for *Candida* hyphal cells to cause damage to epithelial cells (14). Another possible reason for the lack of a phenotype in the cryptococcal development of the *dha2*Δ mutant might be due to functional redundancy. Functional redundancy has been shown to prevail in the *FLO* gene family of *Saccharomyces* during various processes such as mating, filamentation, and flocculation (8). Alternatively, it is possible that the increased *DHA2* gene expression level during cryptococcal development does not correlate with its protein level and that there is a dichotomy in *DHA2* gene expression and Dha2 protein production.

Dha1 and Dha2 have distinct localization patterns during cryptococcal development. Based on the expression profile, the *DHA2* and *CFL1* genes had high transcript levels during cryptococcal sexual development on V8 medium, whereas the *DHA1* gene was highly expressed during yeast-phase growth on YPD medium. In contrast, the transcript levels of *CPL1* remained constant on YPD and V8 media, and the transcript levels of both *CFL105* and *CPL1* were low during culture on either YPD or V8 medium (Fig. 2A). Hence, we decided to focus on the protein expression and localization patterns of *DHA1*, *DHA2*, and *CFL1* during yeast growth and during sexual development on V8 agar medium. For this purpose, we tagged these proteins with mCherry at the C terminus and used their own native promoters to drive their gene expression. Cfl1 fused with mCherry driven by its own promoter (P_{CFL1}-*CFL1*-mCherry) was used as a positive control for a hypha-specific protein (17, 18). When the P_{CFL1}-*CFL1*-mCherry strain was grown on YPD medium, we could not detect the Cfl1-mCherry signal at the colony level or with individual yeast cells (Fig. 5A and B). This observation was consistent with its smooth colony morphology as well as the extremely low transcript level of *CFL1* under this condition (Fig. 2A and 4A). When the P_{DHA1}-*DHA1*-mCherry strain was grown on YPD medium, we easily detected the Dha1-mCherry signal in yeast intracellular punctate structures that were consistent with secretory vesicles (Fig. 5B). This was consistent with the high transcript level of *DHA1* during yeast growth (Fig. 2A and 4A). Likewise, we easily detected the Dha2-mCherry signal in vesicles in yeast cells (Fig. 5B).

Next, we examined their localization during sexual development on V8 agar medium. The *Cryptococcus* mating colony is heterogeneous in morphology, and it consists

of cell types including yeast, aerial hyphae, and invasive hyphae. Later during sexual development, some of the aerial hyphae go on to produce basidia, where meiosis and sporulation take place. Based on the fluorescence image of the mating colony, the Cfl1 and Dha2 proteins were abundantly produced when cells were grown on V8 medium, whereas a much-reduced signal of Dha1 was detected at the colony level under the same conditions (Fig. 5A). At the cellular level, Cfl1 was highly expressed in hyphae but rarely in yeasts, and Cfl1 was observed in structures consistent with secretory vesicles (Fig. 5B). Surprisingly, although *DHA2*, like *CFL1*, had high transcript levels when *Cryptococcus* cells were cultured on V8 medium, the Dha2 protein was detected mostly in yeast cells (Fig. 5B) and rarely in hyphal cells. This Dha2 protein expression pattern on V8 medium was opposite that of Cfl1. Thus, our data indicate that the gene expression profile at the population level is not always indicative of the behaviors of individual cell types within a heterogeneous population. The transcript level of *DHA1* was low on V8 medium. Consistently, only some yeast cells showed a weak signal for Dha1-mCherry in intracellular punctate structures during early developmental stages of *Cryptococcus* (Fig. 5B). Interestingly, Dha1-mCherry was localized at the basidium neck and in spores at a later stage during sexual development (Fig. 5B). This finding suggests that Dha1 is also a spore protein.

Our observations indicate cell type-specific expression patterns of the Cfl1 family proteins. Cfl1 is specific to hyphae, whereas Dha1 is enriched in yeasts, basidia, and spores. In contrast, Dha2 is specific to yeast cells. Hence, the unique expression pattern of Dha1, Dha2, and Cfl1 may contribute to the heterogeneity of the cell surface and physiology within a mating population of *Cryptococcus*. Our data also suggest that gene expression data from a whole population should be interpreted with caution due to the existence of heterogeneous subpopulations.

Dha1 is responsive to copper limitation. Dha1 was highly expressed by yeast cells in YPD medium but not by yeast cells cultured on V8 medium. We previously found that YPD medium was copper limiting to *Cryptococcus*, as the copper transcription factor *mac1*Δ (also known as *cuf1*Δ) mutant grew poorly on YPD medium without copper supplementation (28). In contrast, copper in V8 medium is a known factor that stimulates cryptococcal filamentation (29). Thus, we decided to examine the influence of copper availability on Dha1 protein production. Here, we cultured the P_{DHA1}-*DHA1*-mCherry strain on YPD medium supplemented with copper or the copper chelator BCS. Remarkably, the Dha1-mCherry fluorescence signal was drastically repressed by even 50 μM copper on YPD medium (Fig. 6A). Consistently, a closer examination at the cellular level showed a similar reduction of the Dha1-mCherry signal in yeast cells in YPD medium supplied with extra copper (Fig. 6B). A drastic repression of Dha1-mCherry by copper was also seen on V8 medium during mating (Fig. 6C). At the colony level, the Dha1-mCherry signal was not detected in the presence of copper, and it was slightly induced by BCS on V8 medium (Fig. 6C). At the cellular level, we did not detect Dha1-mCherry on the neck of the basidium when copper was added (Fig. 6D). We also noticed a reduction in basidium production in the presence of extra copper in the medium, even though filamentation was increased (29).

To test if the fluorescence reduction seen in the P_{DHA1}-*DHA1*-mCherry strain is a general effect of copper, we examined the impact of copper on the Dha2-mCherry signal from the P_{DHA2}-*DHA2*-mCherry strain cultured in YPD medium. We did not observe dramatic copper-dependent repression (Fig. 6A and B). We also examined the effect of copper on the expression of the hypha-specific protein Cfl1-mCherry. The Cfl1 signal from the P_{DHA1}-*DHA1*-mCherry strain cultured on V8 medium was not affected by the presence of either copper or the copper chelator (Fig. 6C). Collectively, these results indicate that Dha1 is responsive to the copper level in the medium.

Impact of the *DHA1* deletion on cryptococcal intracellular replication in macrophages. *Cryptococcus* experiences a copper-limiting environment in macrophages and during brain infection but not in the lungs (30). Since our results showed that Dha1 was highly produced during copper limitation, we examined if the deletion of *DHA1*

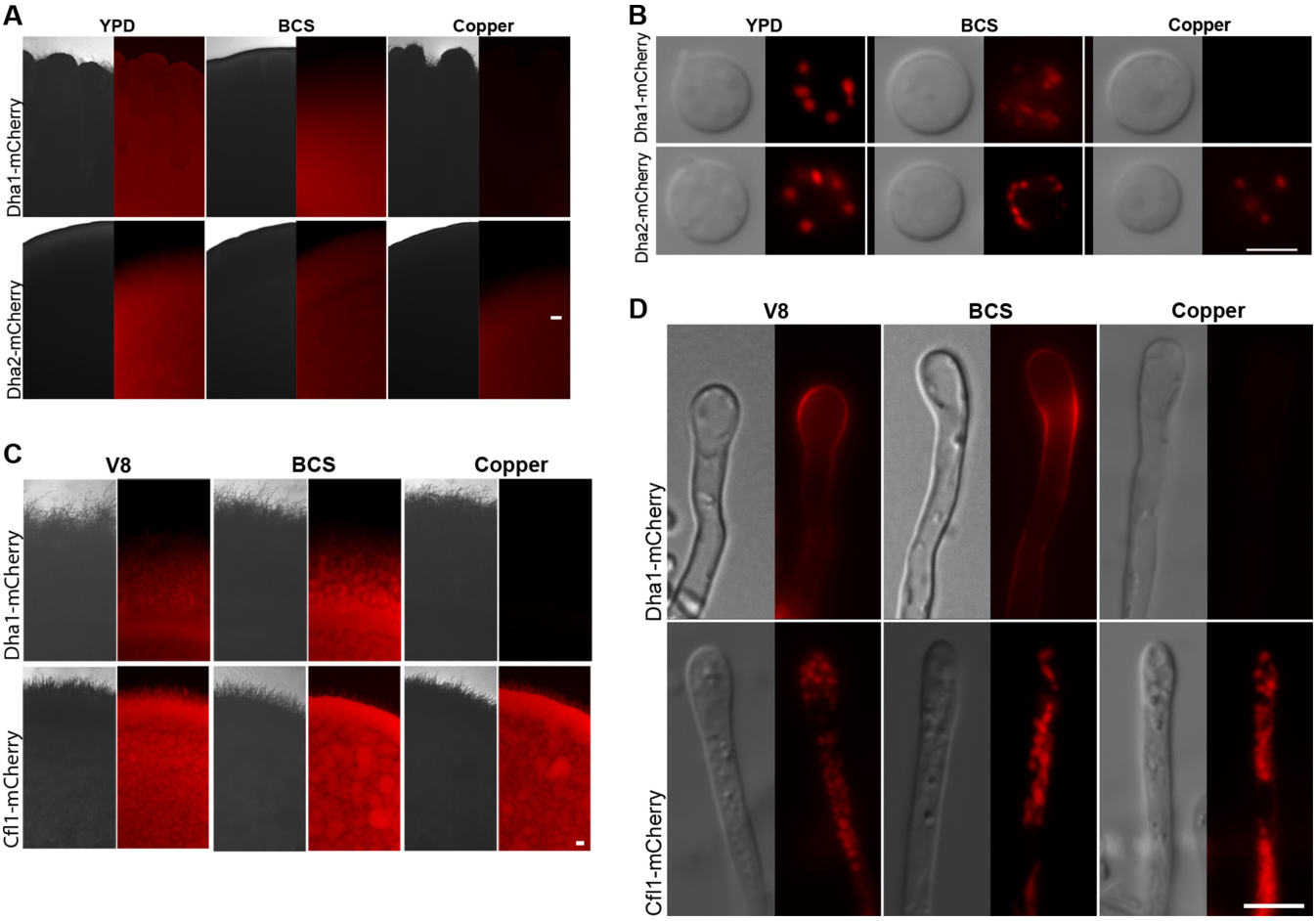

FIG 6 Dha1 is repressed by copper. Cells of the P_{CFL1}-*CFL1*-mCherry strain, the P_{DHA1}-*DHA1*-mCherry strain, and the P_{DHA2}-*DHA2*-mCherry strain were spotted onto YPD or V8 agar medium with or without the addition of copper or the copper chelator BCS. (A and C) Colony images were taken after 5 days for strains grown on YPD medium (A) or after 10 days for strains grown on V8 medium (C). (B and D) Images of yeast cells cultured in YPD medium (B) and images of hyphal cells from colonies on V8 medium (D). Bars, 100 μm (A and C) and 5 μm (B and D).

had any effect on intracellular replication within macrophages. For the phagocytosis assay, cryptococcal cells were coincubated with macrophages for 2 h before nonadherent *Cryptococcus* cells were removed by thorough washing. We then added the fungistatic drug fluconazole to inhibit the replication of extracellular cryptococcal cells, as described previously (31, 32). After 24 h of coincubation, we measured the intracellular and extracellular fungal burdens by counting cryptococcal CFU present in the medium alone versus cryptococcal CFU from lysed macrophages. As a control, we also examined the growth of the wild type, the *dha1*Δ mutant, or the reconstituted strain cultured under the same conditions without macrophages. For the control samples, there was no difference in growth between the wild type, the *dha1*Δ mutant, or the reconstituted strain without macrophages (see Fig. S4 in the supplemental material). For the macrophage assay, we found no difference between the *dha1*Δ mutant, the wild type, and the complemented strain 2 h after coculture with macrophages (Fig. 7A). This finding suggests that the deletion of the *DHA1* gene does not affect initial cryptococcal phagocytosis or adherence. We detected a modest trend in the reduction of CFU of the *dha1*Δ mutant in the intracellular pool after 24 h of coculture with macrophages, but this trend is not statistically significant. The extracellular pool of the *dha1*Δ mutant was similar to that of the wild type at this time point (Fig. 7B and C). The reconstituted strain showed no difference in intracellular CFU compared to the wild type. The *dha1*Δ mutant in the H99 background showed a statistically significant but very slight reduction in intracellular CFU compared to the H99 control, while no

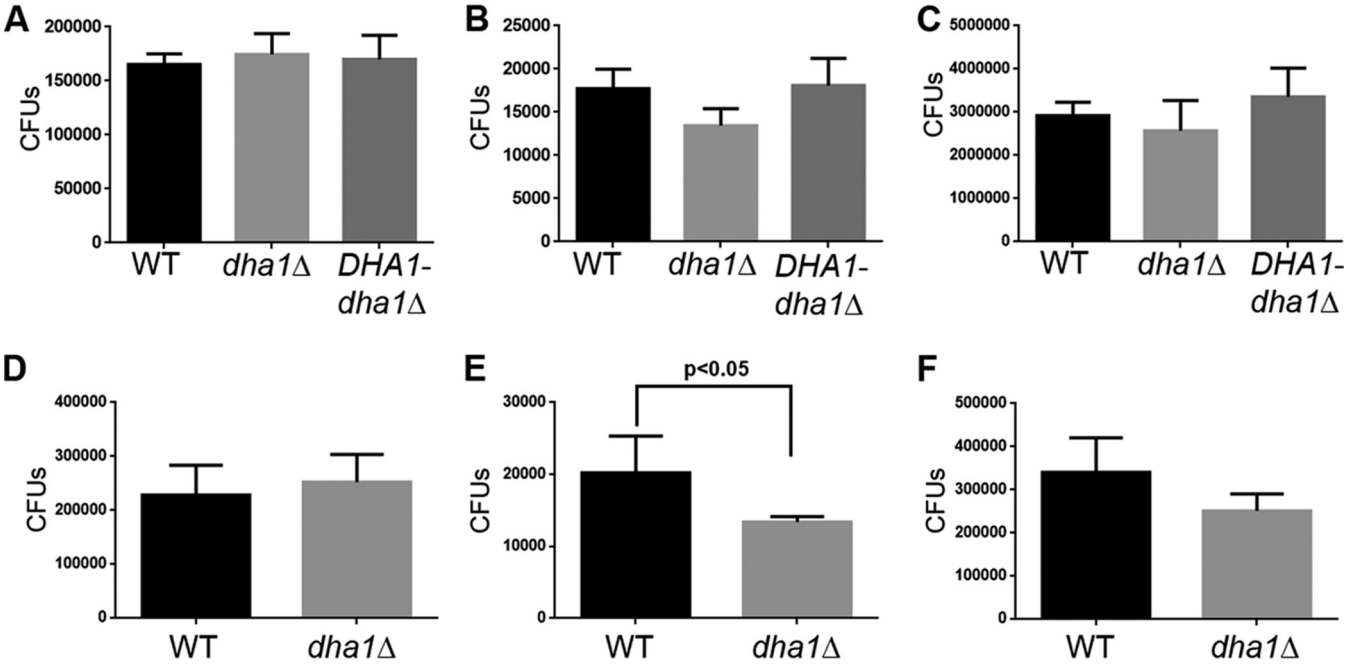

FIG 7 (A to C) The *dha1*Δ mutant has reduced intracellular survival or replication. *Cryptococcus* cells of the wild type, the *dha1*Δ mutant, and the Dha1-reconstituted strain in the XL280 background were opsonized in mouse serum for 30 min. These strains were then incubated with macrophages for 2 h or 24 h at 37°C in 5% CO_2. (A) Numbers of adherent cells and the original phagocytosed *Cryptococcus* cells were determined after the initial 2 h of incubation with macrophages. (B) CFU of intracellular cryptococcal cells at 24 h of coculture with macrophages were obtained from lysed macrophage cells after washing. (C) CFU of extracellular *Cryptococcus* cells at 24 h of coculture with macrophages were obtained from the extracellular medium containing the fungistatic drug fluconazole. (D to F) Similarly, determinations of adherence (D), intracellular CFU (E), and extracellular CFU (F) for WT strain H99 and the *dha1*Δ mutant in the H99 background were performed similarly but without opsonization.

difference in phagocytosis or the extracellular pool between the *dha1*Δ mutant and H99 was observed (Fig. 7D to F).

DISCUSSION

In this study, we showed that all four homologs of Cfl1 in *Cryptococcus* are secretory proteins and are released extracellularly, similarly to Cfl1 (18). A BLAST search of the C-terminal SIGC domain against the fungal kingdom showed that this protein family is conserved among some diverse species in the Basidiomycota (see Fig. S5 in the supplemental material). This family of secretory proteins might be involved in diverse biological functions of this fungus. For instance, the deletion of *CPL1* affects cryptococcal capsule formation, a major virulence factor of this pathogen. The deletion of *DHA1* may affect the cryptococcal response to copper. Characterization of secretory proteins might help future vaccine or diagnostic research. For instance, Dha1 is named for its ability to cause delayed-type hypersensitivity (20), and Cpl1 can be detected in serum of mice infected with a *Cryptococcus neoformans* isolate (22).

One interesting and important finding of this study is the cell type specificities shown by some of these homologs (Fig. 8). Cfl1 was previously shown to be a hypha-specific protein (17, 18). Consistently, the transcript level of *CFL1* is significantly increased during sexual development with Cfl1 proteins produced by hyphae but not by yeast cells. Dha1, on the other hand, is expressed in multiple cell types, with stronger expression in yeast cells and weaker expression in filaments but with specific enrichment on the neck of the basidium and in spores (Fig. 8). Intriguingly, Dha1 is induced by copper limitation and repressed by copper. The Dha1 protein is cysteine rich (6.7%). In comparison, the housekeeping proteins Tef1 (8/459), Gpd1 (4/344), and Act1 (5/377) have only 1.7%, 1.16%, and 1.3% of their residues being cysteine, respectively. It is possible that Dha1 plays a role in sensing the redox status of its environment, which connects to its response to the copper level in the environment. One of the most surprising findings of this study is the dichotomy between the protein expression

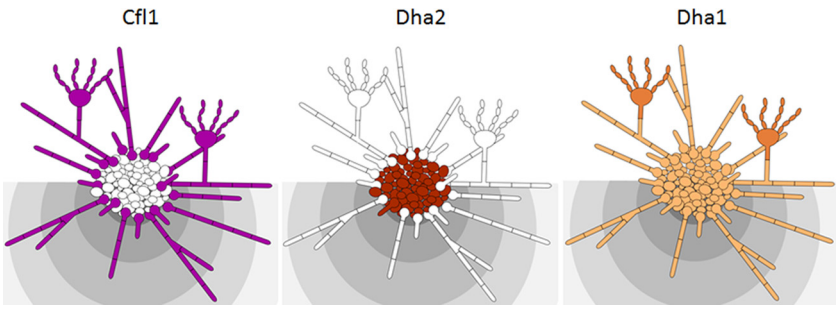

FIG 8 Cell type-specific expression pattern shown by Cfl1, Dha1, and Dha2 during sexual development. Cfl1 is produced by hyphae, whereas Dha2 is produced mostly by yeast cells. Dha1 is weakly expressed in yeast cells during mating on V8 medium. However, it is enriched in basidia and spores.

pattern of Dha2 and its transcript pattern. Like *CFL1*, the *DHA2* transcript level is high under mating conditions. We thus expected that Dha2 was going to be a hypha-specific protein. Surprisingly, the Dha2 protein is expressed only by the yeast and not by the hyphal subpopulation of the mating colony (Fig. 8). The expression level of *CFL105* is low in all our RNA-seq data (23; our unpublished data). Based on previously reported RNA-seq data (33), the *CFL105* level is only modestly increased during stationary growth compared to exponential growth (33), and its biological function remains unclear. Although transcript data obtained during sexual development are useful and have been used widely to identify genes that are potentially important for development and morphogenesis, it is important not to assume a protein's function based purely on the transcript data collected from a heterogeneous population.

The cell type-specific expression shown by cell surface or secretory proteins is not uncommon. Morphological transitions in microbes are associated with changes in the expression of cell surface proteins (6). The changes in the expression levels of secretory proteins contribute to the diversity in physiology of cells of different morphotypes (6). The observation that high levels of Dha2 are present only in yeast cells during sexual development suggests that it might be important for maintaining heterogeneity in the community. We noticed that all of the cells that express Dha2 were round yeast cells and not shmoo cells or germ tubes. This intriguing observation suggests that Dha2-producing cells might not be producing or responding to pheromones. This difference in physiology might allow some cells to further differentiate into hyphae while maintaining a subpopulation of yeast cells in a mating colony. Combining the high expression levels of Dha1 in yeasts and spores, Dha2 in yeasts, and Cfl1 in hyphae, the expression pattern of multiple surface and secretory proteins confers diverse properties to the mating colony of *Cryptococcus*, which contains a population with heterogeneous morphotypes. This bet-hedging strategy might help the population cope with unforeseeable environment changes.

MATERIALS AND METHODS

Strains and growth conditions. Strains used in this study are listed in Table 1. *Cryptococcus* strains were stored at −80°C and grown on YPD medium for routine culture. Mating assays were performed on V8 (pH 7) medium at 22°C in the dark.

Generation of gene disruption and overexpression strains. Primers used in this study are listed in Table 2. Gene deletion was conducted by using the split-marker recombination strategy as described previously (34). Briefly, the 5′- and 3′-flanking regions of the gene of interest were fused to two-thirds of the fragment of the nourseothricin (NAT) or the geneticin (NEO) dominant drug resistance marker by using overlap PCR. Two split fragments were mixed and introduced into *Cryptococcus neoformans* by using biolistic transformation as described previously (35). Transformants with a gene deletion were confirmed by PCR. To verify that any phenotype observed, or the lack thereof, was genetically linked to the gene deletion, we crossed each of our deletion mutants made in the α background with the congenic wild-type **a** strain (36). We then dissected meiotic basidiospores using a tetrad micromanipulator and performed a genetic linkage assay by phenotyping/genotyping of the dissected meiotic progeny. This approach allowed us to verify that the gene deletion was segregating in the Mendelian fashion. Furthermore, this approach allowed us to obtain the gene deletion mutants in the **a** mating type and to analyze their phenotypes as described previously (36). These mutants in the mating type **a** background

TABLE 1 Strains used in this study

Strain	Genotype	Reference or source	Background
KN99**a**	*MAT***a** (WT)	40	H99
KN99α	*MAT*α (WT)	40	H99
XL280α	*MAT*α (WT)	28	XL280
XL280**a**	*MAT***a** (WT)	27	XL280
	*MAT*α *dha1*::*NAT*	H. D. Madhani, FGSC	H99
	*MAT*α *dha2*::*NAT*	H. D. Madhani, FGSC	H99
	*MAT*α *cpl1*::*NAT*	H. D. Madhani, FGSC	H99
	*MAT*α *cfl105*::*ss*	H. D. Madhani, FGSC	H99
BZ30α	*cfl1*::*HYG*	This study	H99
LW303α	P_{CTR4}-*CFL1*::*mCherry*(*sigP*Δ)::*NEO*^{r}	17	H99
RG249α	P_{CTR4}-*DHA1*::*mCherry*::*NEO*^{r}	This study	H99
RG264α	P_{CTR4}-*CPL1*::*mCherry*::*NEO*^{r}	This study	H99
RG251α	P_{CTR4}-*CFL105*::*mCherry*::*NEO*^{r}	This study	H99
RG425α	P_{CTR4}-*DHA2*::*mCherry*::*NEO*^{r}	This study	H99
LW204α	P_{CTR4}-*CFL1*::*mCherry*::*NEO*^{r}	17	H99
RG48α	*dha1*::*NEO*	This study	XL280
RG117α	*dha2*::*NAT*	This study	XL280
RG212α	*cpl1*::*NEO*	This study	XL280
RG192α	*cfl105*::*NEO*	This study	XL280
XL1359α	*cfl1*::*NEO*	17	XL280
RG107α	*dha1*::*NAT*	This study	H99
RG83α	P_{DHA1}-*DHA1*::*mCherry*::*NEO*^{r}	This study	XL280
RG153α	P_{DHA2}-*DHA2*::*mCherry*::*NEO*^{r}	This study	XL280
LW192α	P_{CFL1}-*CFL1*::*mCherry*::*NEO*^{r}	17	XL280
RG52**a**	*dha1*::NEO	This study	XL280
RG182**a**	*dha2*::*NAT*	This study	XL280
JW7**a**	*cpl1*::*NEO*	This study	XL280
JW1**a**	*cfl105*::*NEO*	This study	XL280
BZXL2**a**	*cfl1*::*NEO*	This study	XL280
LW799α	*cfl1*::*NEO* P_{CFL1}-*CFL1*::*HYG*	This study	XL280
RG453α	*dha1*::NEO P_{DHA1}-*DHA1*::*mCherry NEO*	This study	XL280

behaved similarly to the corresponding mutants in the mating type α background. For the construction of the overexpression vector, an amplified fragment of the open reading frame (ORF) of the gene was digested and ligated into the pXL1-mCherry plasmid after the *GPD1* promoter or the *CTR4* promoter (17). The *GPD1* promoter was used for constitutive expression. The *CTR4* promoter was used as an inducible system, with the copper chelator BCS inducing the expression of the gene and copper repressing the expression of the gene. The vector also contains the mCherry tag toward the C terminus of the gene, as described previously (17). The overexpression construct was then introduced into *Cryptococcus neoformans* strains by using biolistic transformation as described previously (35).

Construction of mCherry-tagged proteins driven by their native promoters. The mCherry-tagged proteins driven by their native promoters were constructed as described previously (17). The gene's ORF together with ~1 kb of upstream sequences were amplified by PCR and ligated into a vector containing mCherry such that mCherry was fused in frame with the C terminus of the gene. The construct was introduced into *Cryptococcus* cells by using biolistic transformation.

Phenotypic assays. Phenotypic assays were performed as described previously (37). Briefly, strains to be tested were grown overnight in YPD liquid medium. The cells were washed and adjusted to the same density (optical density at 600 nm [OD_{600}] of 3). For thermotolerance assays, cells were serially diluted, spotted onto YPD agar medium, and incubated at 30°C, 37°C, or 39°C. For the capsule formation assay, cells were cultured in liquid fetal bovine serum (FBS) or in RPMI medium for 48 h at 37°C with 5% CO_2. The capsule was visualized as a halo surrounding the yeast cell under a light microscope through India ink exclusion. Melanin production was visualized by spotting the cells onto L-DOPA (L-dihydroxyphenylalanine) medium. For mating assays, cells were incubated on V8 medium in the dark at 22°C for 3 days before the mating filament images were taken. Colony images were taken on day 5 after incubation at 22°C with an Olympus SZX16 stereoscope. To visualize basidia and spore chains, cells were incubated on V8 medium for 10 to 14 days, and images were taken by using a Zeiss AxioCam 506 camera.

For cell adherence assays, strains were cultured in different growth media, such as YPD solid medium, YNB solid medium, or RPMI liquid medium, with either BCS or copper (for the induction or the suppression of genes controlled by the *CTR4* promoter, respectively). For invasive growth assays, cells were cultured on YNB solid medium for 3 days. Loose cells were washed off with water three times before invasive cells were photographed. To examine cell adherence to glass, cells were cultured in liquid RPMI medium on a glass slide with either BCS or copper for 4 days at 37°C. The glass slide was washed three times with water before the slides were observed for adherent cells under a microscope. Images of the cells were captured with an AxioCam 506 camera connected to a Zeiss Imager M2 microscope. Colony morphology was observed under an Olympus SZX16 stereoscope. Colonies before and after washing

TABLE 2 Primers used in this study

Purpose or target	Primer	Primer sequence
DHA1 deletion in XL280	Linlab1227	CTCAGACAGCAGGACAGAGC
	Linlab1229	GTCATAGCTGTTTCCTGCGGCAAAAATCTGTATCCC
	Linlab1230	AGATTGACATTGTGGTCCTCA
	Linlab1232	ATGTTCTCGTCCACTATTGC
	Linlab1233	CAGACTTGGTGCACTCGC
	Linlab1587	GAACGAACCCTTTTCAAACA
	Linlab1588	CTGACTGCTGGAAACTGAAAAC
	Linlab1589	CTGGCCGTCGTTTTACTTGTTTGCGTTGTTGTTGTC
	Linlab1677	GTAGTCCCTGAACCCTCTAAT
	Linlab1678	TGATACTCGTATCCACTGCTG
DHA2 deletion in XL280	Linlab1418	CGGAAAGCAGCTGCATATAAG
	Linlab1419	CTGGCCGTCGTTTTACGAGTGAGGTTGAAAAGAATGAGTGTAGT
	Linlab1420	GTCATAGCTGTTTCCTGGTCTTACCGTCGCTTTCTATATCG
	Linlab1421	CACTTCTTTTGCCCCGAAACT
	Linlab1422	CGGGGTACAAGAGGAAACAGC
	Linlab1676	ACTGATGGAAGGTTACAAGAC
CPL1 deletion in XL280	Linlab2520	TTATCATGCTCCCTGTTCC
	Linlab2521	AATTATTGCCCTAAAGGGAG
	Linlab2522	AGCCACTCGTTCAAATTTAC
	Linlab2523	GTGCCTGGAAAGTCTTCTCA
	Linlab2524	CTGGCCGTCGTTTTACGGAAGAGTTTTTGGCAAGTT
	Linlab2525	GTCATAGCTGTTTCCTGGTGCCTTTATAGAAGCCACT
	Linlab2526	ATAACACCGGCTTTGATGTC
	Linlab2527	ATTGCGTCGTACTGGTCAC
CFL105 deletion in XL280	Linlab2531	GATAATAGCCATGTTCCTTTC
	Linlab2532	GTCTCTCACACTCAGTCCCAT
	Linlab2533	ACAATGTCAGAACCTCTGGT
	Linlab2534	ACCCTTTCCACTATAGATCC
	Linlab2535	CTGGCCGTCGTTTTACGAGCAAAAGGACTGTATCG
	Linlab2536	GTCATAGCTGTTTCCTGTCGATTTTATGACCAGACG
	Linlab2537	AAGACGGGGTCTCTCAAAC
	Linlab2538	CCTCTTCTGGTCAGACAATA
DHA1 deletion in H99	Linlab1970	CGACGGAAGACTAGATCAATAA
	Linlab1971	CTGGCCGTCGTTTTACATGAGGTGGTAAGGAAGAATG
	Linlab1972	GTCATAGCTGTTTCCTGCTGATCTGCTGTTTCATTTAGG
	Linlab1973	CAGCTGGAGAGTGACAGACTTG
	Linlab1974	CTGGATTCTAATGTACTCAGCT
	Linlab1975	ACTCCCACGACAACAACAAC
	Linlab1976	TGGCACTGTCACTCTGTCTAC
	Linlab1977	AGCAGAGGGAAAAGTGACGTAC
Cfl105^{oe} P_{CTR4}*CFL105*-mCherry	Linlab2539	CCGGCCGGCCATGTTCCTTTCCCCCATCT
	Linlab2541	GATTCACGCGATCGCTAATAGTCTCTCACACTCAGTC
Cpl1^{oe} P_{CRT4}*CPL1*-mCherry	Linlab2528	CCGGCCGGCCATGCTCCCTGTTCCTCCCT
	Linlab2530	GATTCACGCGATCGCTTGCCCTAAAGGGAGCTGA
P_{DHA1}*DHA1*-mCherry	Linlab1797	ATCTTAAGCGGCCGCCGGTGTTGATCGTTTAGCTTT
	Linlab1798	GATTCACGCGATCGCCAGCTGGAGAGTGACAGA
P_{DHA2}*DHA2*-mCherry	Linlab1731	GTACAATGCGATCGCCAACTGGAACGTAAAGGTT
	Linlab1799	ATCGTTAGCGGCCGCCTAGGGATGAAACTCGTGAAG
Dha1^{oe} P_{CTR4}*DHA1*-mcherry	Linlab1966	CCGGCCGGCCATGTTCTCGTCCACTATTGCG
	Linlab2236	CCTTAATTAACAGCTGGAGAGTGACAGA
Dha2^{oe} P_{CTR4}*DHA2*-mcherry	Linlab1967	CCGGCCGGCCATGTACTCTTCCGCCATCATG
	Linlab2237	CCTTAATTAACAACTGGAACGTAAAGGTT
DHA1 (RT-PCR)	Linlab2280	TTGACCCTACTTCCGATATC
	Linlab2281	CAAAGGCTTCACATCGACT

(Continued on next page)

TABLE 2 (Continued)

Purpose or target	Primer	Primer sequence
DHA2 (RT-PCR)	Linlab2314	GACCCTACTACGGAACTTGA
	Linlab2315	GAAGGCCTCACATTTGCT
CPL1 (RT-PCR)	Linlab2291	CCAGGCGATGAAGTTTCT
	Linlab2292	CAGAACCAAGTGCTAAGCA
CFL105 (RT-PCR)	Linlab2293	ATCTGGCACCAGGAATGA
	Linlab2294	GCTCACTGCATCTCCATCT
CFL1 (RT-PCR)	Linlab795	GGTCTCTCCATGCTTGTACC
	Linlab796	CCAGATTTGCAGCTGTAGAC
TEF1 (RT-PCR)	Linlab329	CGTCACCACTGAAGTCAAGT
	Linlab330	AGAAGCAGCCTCCATAGG

were observed with an Olympus SZX16 stereoscope, and images were captured by using a Zeiss AxioCam 506 camera.

For examining protein subcellular localization, strains were grown on YPD or V8 medium. The cells were visualized by using a Zeiss Imager M2 fluorescence microscope with an AxioCam 506 camera. The filter used for visualizing mCherry was the 43 HE cy3 FL filter set (Carl Zeiss Microscopy). To observe protein localization at various stages of cryptococcal development, cells were visualized at different time points after incubation on V8 agar medium.

RNA purification and quantitative PCR. RNA extraction and quantitative RT-PCR were performed as described previously (17). Cells undergoing unisexual development on V8 medium were harvested at various time points as indicated in the figures, washed with cold double-distilled water (ddH_2O), and lyophilized. Total RNA was extracted by using the PureLink RNA minikit from Life Technology according to the manufacturer's instructions. After DNase I treatment, the samples were analyzed on a formaldehyde agarose gel to assess the RNA quality and concentration. First-strand cDNA synthesis was carried out by using a Superscript III cDNA synthesis kit (Life Technology) according to the manufacturer's instructions. The constitutively expressed housekeeping gene *TEF1* was used as an internal control for the normalization of other genes, as we described previously (17).

Colony immunoblotting. Immunoblotting was performed as we described previously (18). The respective strains were grown overnight in YPD medium. Three microliters of the cell suspension at a density 2×10^7 cells/ml was spotted onto V8 medium and incubated for 5 days at 22°C. A sterile nitrocellulose membrane (Millipore) was then laid over the colonies, and the cells were incubated for an additional 3 days. The membrane was then removed and washed with 1× Tris-buffered saline to remove the attached cells. The blot was then incubated with anti-mCherry primary antibody (1/2,000 dilution; Clontech). A rabbit anti-mouse secondary antibody coupled with horseradish peroxidase (HRP) was then used (1/10,000 dilution; Clontech Inc.). For detection, an enhanced chemiluminescence (ECL) system was used according to the manufacturer's instructions (Pierce).

Phagocytosis assay. The mouse macrophage cell line J774A.1 (ATCC TIB-67) was used for the phagocytosis assay as described previously (38). Macrophage cells were cultured in Dulbecco's modified Eagle's medium (DMEM; catalog no. 30-2002) with 10% FBS. *Cryptococcus* WT strain XL280, the *dha1*Δ mutant, and the reconstituted strain were used for this study. *Cryptococcus* cells were opsonized with mouse serum at 37°C for 30 min as previously described (39). Freshly grown J774A.1 cells were seeded into a 24-well microtiter plate overnight at 37°C in 5% CO_2, with each well containing 2.5×10^5 *Cryptococcus* cells per 500 μl. The next day, the medium in each well was replaced with fresh medium containing 2.5×10^6 *Cryptococcus* cells in 500 μl of medium. The cryptococcal cells were mixed well with the macrophage cells by rocking for 30 s and were incubated at 37°C in 5% CO_2. After 2 h, the cocultures were washed with phosphate saline buffer (500 μl per well) 6 times to remove nonadherent cells. The numbers of adherent cells were measured by using duplicated cocultures. The cocultures were further incubated in fresh medium (DMEM with 10% FBS) containing fluconazole (5 μg/ml) for 24 h. Fluconazole was added to inhibit the extracellular replication of *Cryptococcus* (31). After 24 h, intracellular and extracellular populations of *Cryptococcus* were measured. For measuring the extracellular population, the cocultures were washed 6 times with phosphate-buffered saline (PBS). This extracellular fluid and its different dilutions were plated onto YNB agar medium, and CFU were measured after an additional 48 h of incubation. The intracellular population of *Cryptococcus* cells was measured by lysing macrophage cells after the extracellular population of *Cryptococcus* was collected. To lyse macrophages, 100 μl of 0.5% Tween 20 was added to the culture, and the mixture was incubated at 37°C for 10 min. The suspension was made up to 200 μl by the addition of YPD medium, serially diluted, and plated onto YNB agar medium. CFU were counted 48 h after incubation at 30°C. A phagocytosis assay was also performed for H99 and its *dha1*Δ mutant according to a procedure similar to the one described above but without opsonization.

Growth rates of the strains used for the phagocytosis assay, namely, WT strain XL280, the *dha1*Δ mutant, and the reconstituted *DHA1-dha1*Δ strain, were measured in DMEM with or without fluconazole. Equal numbers of cells (500 cells) were grown in DMEM at 37°C in 5% CO_2 with or without the addition

of fluconazole. After 24 h, cells were serially diluted and plated onto YNB agar medium. CFU were counted after 24 h of incubation at 30°C.

SUPPLEMENTAL MATERIAL

Supplemental material for this article may be found at https://doi.org/10.1128/AEM.02967-16.

TEXT S1, PDF file, 0.9 MB.

ACKNOWLEDGMENTS

We thank Linqi Wang and Lin laboratory members for their helpful suggestions. We also thank Jianfeng Lin for his help with the macrophage assay.

This work was supported by the National Institutes of Health (grants R01AI097599 and R21AI107138 to X.L.). X.L. holds an investigator award in the pathogenesis of infectious disease from the Burroughs Wellcome Fund (http://www.bwfund.org/). The funders had no role in study design, data collection and interpretation, or the decision to submit the work for publication.

R.G., S.U., and X.L. conceived of and designed the experiments; R.G., S.U., and J.W. performed the experiments; R.G., S.U., and X.L. analyzed the data; X.L. contributed reagents/materials/analysis tools; and R.G. and X.L. wrote the paper.

REFERENCES

1. Verstrepen KJ, Fink GR. 2009. Genetic and epigenetic mechanisms underlying cell-surface variability in protozoa and fungi. Annu Rev Genet 43:1–24. https://doi.org/10.1146/annurev-genet-102108-134156.
2. de Groot PWJ, Bader O, de Boer AD, Weig M, Chauhan N. 2013. Adhesins in human fungal pathogens: glue with plenty of stick. Eukaryot Cell 12:470–481. https://doi.org/10.1128/EC.00364-12.
3. Sundstrom P. 2002. Adhesion in *Candida* spp. Cell Microbiol 4:461–469. https://doi.org/10.1046/j.1462-5822.2002.00206.x.
4. Ramage G, Martínez JP, López-Ribot JL. 2006. *Candida* biofilms on implanted biomaterials: a clinically significant problem. FEMS Yeast Res 6:979–986. https://doi.org/10.1111/j.1567-1364.2006.00117.x.
5. Sahni N, Yi S, Daniels KJ, Srikantha T, Pujol C, Soll DR. 2009. Genes selectively up-regulated by pheromone in white cells are involved in biofilm formation in *Candida albicans*. PLoS Pathog 5:e1000601. https://doi.org/10.1371/journal.ppat.1000601.
6. Verstrepen KJ, Klis FM. 2006. Flocculation, adhesion and biofilm formation in yeasts. Mol Microbiol 60:5–15. https://doi.org/10.1111/j.1365-2958.2006.05072.x.
7. Reynolds TB, Fink GR. 2001. Bakers' yeast, a model for fungal biofilm formation. Science 291:878–881. https://doi.org/10.1126/science.291.5505.878.
8. Guo B, Styles CA, Feng Q, Fink GR. 2000. A *Saccharomyces* gene family involved in invasive growth, cell-cell adhesion, and mating. Proc Natl Acad Sci U S A 97:12158–12163. https://doi.org/10.1073/pnas.220420397.
9. Nobile CJ, Schneider HA, Nett JE, Sheppard DC, Filler SG, Andes DR, Mitchell AP. 2008. Complementary adhesin function in *C. albicans* biofilm formation. Curr Biol 18:1017–1024. https://doi.org/10.1016/j.cub.2008.06.034.
10. Ene IV, Bennett RJ. 2009. Hwp1 and related adhesins contribute to both mating and biofilm formation in *Candida albicans*. Eukaryot Cell 8:1909–1913. https://doi.org/10.1128/EC.00245-09.
11. Hayek P, Dib L, Yazbeck P, Beyrouthy B, Khalaf RA. 2010. Characterization of Hwp2, a *Candida albicans* putative GPI-anchored cell wall protein necessary for invasive growth. Microbiol Res 165:250–258. https://doi.org/10.1016/j.micres.2009.03.006.
12. Granger BL, Flenniken ML, Davis DA, Mitchell AP, Cutler JE. 2005. Yeast wall protein 1 of *Candida albicans*. Microbiology 151:1631–1644. https://doi.org/10.1099/mic.0.27663-0.
13. Granger BL. 2012. Insight into the antiadhesive effect of yeast wall protein 1 of *Candida albicans*. Eukaryot Cell 11:795–805. https://doi.org/10.1128/EC.00026-12.
14. Moyes DL, Wilson D, Richardson JP, Mogavero S, Tang SX, Wernecke J, Höfs S, Gratacap RL, Robbins J, Runglall M, Murciano C, Blagojevic M, Thavaraj S, Förster TM, Hebecker B, Kasper L, Vizcay G, Iancu SI, Kichik N, Häder A, Kurzai O, Luo T, Krüger T, Kniemeyer O, Cota E, Bader O, Wheeler RT, Gutsmann T, Hube B, Naglik JR. 2016. Candidalysin is a fungal peptide toxin critical for mucosal infection. Nature 532:64–68. https://doi.org/10.1038/nature17625.
15. Brandhorst T, Wuthrich M, Finkel-Jimenez B, Klein B. 2003. A C-terminal EGF-like domain governs BAD1 localization to the yeast surface and fungal adherence to phagocytes, but is dispensable in immune modulation and pathogenicity of *Blastomyces dermatitidis*. Mol Microbiol 48:53–65. https://doi.org/10.1046/j.1365-2958.2003.03415.x.
16. Tian X, Lin X. 2013. Matricellular protein Cfl1 regulates cell differentiation. Commun Integr Biol 6:e26444. https://doi.org/10.4161/cib.26444.
17. Wang L, Zhai B, Lin X. 2012. The link between morphotype transition and virulence in *Cryptococcus neoformans*. PLoS Pathog 8:e1002765. https://doi.org/10.1371/journal.ppat.1002765.
18. Wang L, Tian X, Gyawali R, Lin X. 2013. Fungal adhesion protein guides community behaviors and autoinduction in a paracrine manner. Proc Natl Acad Sci U S A 110:11571–11576. https://doi.org/10.1073/pnas.1308173110.
19. Hoyer LL. 2001. The ALS gene family of *Candida albicans*. Trends Microbiol 9:176–180. https://doi.org/10.1016/S0966-842X(01)01984-9.
20. Mandel MA, Grace GG, Orsborn KI, Schafer F, Murphy JW, Orbach MJ, Galgiani JN. 2000. The *Cryptococcus neoformans* gene *DHA1* encodes an antigen that elicits a delayed-type hypersensitivity reaction in immune mice. Infect Immun 68:6196–6201. https://doi.org/10.1128/IAI.68.11.6196-6201.2000.
21. Liu OW, Chun CD, Chow ED, Chen C, Madhani HD, Noble SM. 2008. Systematic genetic analysis of virulence in the human fungal pathogen *Cryptococcus neoformans*. Cell 135:174–188. https://doi.org/10.1016/j.cell.2008.07.046.
22. Cai J-P, Liu L-L, To KKW, Lau CCY, Woo PCY, Lau SKP, Guo Y-H, Ngan AHY, Che X-Y, Yuen K-Y. 2015. Characterization of the antigenicity of Cpl1, a surface protein of *Cryptococcus neoformans* var. *neoformans*. Mycologia 107:39–45. https://doi.org/10.3852/14-074.
23. Chacko N, Zhao Y, Yang E, Wang L, Cai JJ, Lin X. 2015. The lncRNA RZE1 controls cryptococcal morphological transition. PLoS Genet 11:e1005692. https://doi.org/10.1371/journal.pgen.1005692.
24. Wickes BL, Mayorga ME, Edman U, Edman JC. 1996. Dimorphism and haploid fruiting in *Cryptococcus neoformans*: association with the alpha-mating type. Proc Natl Acad Sci U S A 93:7327–7331. https://doi.org/10.1073/pnas.93.14.7327.
25. Lin X, Hull CM, Heitman J. 2005. Sexual reproduction between partners of the same mating type in *Cryptococcus neoformans*. Nature 434:1017–1021. https://doi.org/10.1038/nature03448.
26. Hull CM, Heitman J. 2002. Genetics of *Cryptococcus neoformans*. Annu Rev Genet 36:557–615. https://doi.org/10.1146/annurev.genet.36.052402.152652.
27. Zhai B, Zhu P, Foyle D, Upadhyay S, Idnurm A, Lin X. 2013. Congenic

strains of the filamentous form of *Cryptococcus neoformans* for studies of fungal morphogenesis and virulence. Infect Immun 81:2626–2637. https://doi.org/10.1128/IAI.00259-13.
28. Lin X, Huang JC, Mitchell TG, Heitman J. 2006. Virulence attributes and hyphal growth of *C. neoformans* are quantitative traits and the *MAT*α allele enhances filamentation. PLoS Genet 2:e187. https://doi.org/10.1371/journal.pgen.0020187.
29. Kent CR, Ortiz-Bermúdez P, Giles SS, Hull CM. 2008. Formulation of a defined V8 medium for induction of sexual development of *Cryptococcus neoformans*. Appl Environ Microbiol 74:6248–6253. https://doi.org/10.1128/AEM.00970-08.
30. Waterman SR, Hacham M, Hu G, Zhu X, Park Y-D, Shin S, Panepinto J, Valyi-Nagy T, Beam C, Husain S, Singh N, Williamson PR. 2007. Role of a *CUF1/CTR4* copper regulatory axis in the virulence of *Cryptococcus neoformans*. J Clin Invest 117:794–802. https://doi.org/10.1172/JCI30006.
31. Qin Q-M, Luo J, Lin X, Pei J, Li L, Ficht TA, de Figueiredo P. 2011. Functional analysis of host factors that mediate the intracellular lifestyle of *Cryptococcus neoformans*. PLoS Pathog 7:e1002078. https://doi.org/10.1371/journal.ppat.1002078.
32. Zhai B, Wu C, Wang L, Sachs MS, Lin X. 2012. The antidepressant sertraline provides a promising therapeutic option for neurotropic cryptococcal infections. Antimicrob Agents Chemother 56:3758–3766. https://doi.org/10.1128/AAC.00212-12.
33. Janbon G, Ormerod KL, Paulet D, Byrnes EJ, III, Yadav V, Chatterjee G, Mullapudi N, Hon C-C, Billmyre RB, Brunel F, Bahn Y-S, Chen W, Chen Y, Chow EWL, Coppée J-Y, Floyd-Averette A, Gaillardin C, Gerik KJ, Goldberg J, Gonzalez-Hilarion S, Gujja S, Hamlin JL, Hsueh Y-P, Ianiri G, Jones S, Kodira CD, Kozubowski L, Lam W, Marra M, Mesner LD, Mieczkowski PA, Moyrand F, Nielsen K, Proux C, Rossignol T, Schein JE, Sun S, Wollschlaeger C, Wood IA, Zeng Q, Neuvéglise C, Newlon CS, Perfect JR, Lodge JK, Idnurm A, Stajich JE, Kronstad JW, Sanyal K, Heitman J, Fraser JA, et al. 2014. Analysis of the genome and transcriptome of *Cryptococcus neoformans* var. *grubii* reveals complex RNA expression and microevolution leading to virulence attenuation. PLoS Genet 10:e1004261. https://doi.org/10.1371/journal.pgen.1004261.
34. Lin X, Chacko N, Wang L, Pavuluri Y. 2015. Generation of stable mutants and targeted gene deletion strains in *Cryptococcus neoformans* through electroporation. Med Mycol 53:225–234. https://doi.org/10.1093/mmy/myu083.
35. Toffaletti DL, Rude TH, Johnston SA, Durack DT, Perfect JR. 1993. Gene transfer in *Cryptococcus neoformans* by use of biolistic delivery of DNA. J Bacteriol 175:1405–1411. https://doi.org/10.1128/jb.175.5.1405-1411.1993.
36. Idnurm A. 2010. A tetrad analysis of the basidiomycete fungus *Cryptococcus neoformans*. Genetics 185:153–163. https://doi.org/10.1534/genetics.109.113027.
37. Lin X, Nielsen K, Patel S, Heitman J. 2008. Impact of mating type, serotype, and ploidy on the virulence of *Cryptococcus neoformans*. Infect Immun 76:2923–2938. https://doi.org/10.1128/IAI.00168-08.
38. Lin J, Idnurm A, Lin X. 2015. Morphology and its underlying genetic regulation impact the interaction between *Cryptococcus neoformans* and its hosts. Med Mycol 53:493–504. https://doi.org/10.1093/mmy/myv012.
39. Santiago-Tirado FH, Peng T, Yang M, Hang HC, Doering TL. 2015. A single protein S-acyl transferase acts through diverse substrates to determine cryptococcal morphology, stress tolerance, and pathogenic outcome. PLoS Pathog 11:e1004908. https://doi.org/10.1371/journal.ppat.1004908.
40. Nielsen K, Cox GM, Wang P, Toffaletti DL, Perfect JR, Heitman J. 2003. Sexual cycle of *Cryptococcus neoformans* var. grubii and virulence of congenic a and α isolates. Infect Immun 71:4831–4841. https://doi.org/10.1128/IAI.71.9.4831-4841.2003.